ISSN : 0974 - 7486 Volume 14 Issue 3

Materials Science

An Indian Journal

Full Paper

MSAIJ, 14(3), 2016 [100-108]

Phase equilibria in the Co-Ti-Zr system at 1023K

G.J.Zhou*, Y.Lou, X.S.Li
School of Mechanical engineering, Hunan institute of Science and Technology, Hunan, Yue-yang, 414006, (CHINA)
E-mail: gjzhoumike@163.com

ABSTRACT

The isothermal section of the Co-Ti-Zr ternary system at 1023K has been investigated by means of diffusion triple together with electron probe microanalysis technique. Series of tie lines and tie-triangles have been determined and the isothermal section at 1023K has been established. 17 three-phase equilibria were observed, namely $Co_3Ti+Co_2Zr+Co_2Ti(h)$, $Co_2Zr+Co_2Ti(h)+Co_2Ti(c)$, $Co_3Ti+Co+Co_2Zr$, $Co_2Zr+CoTi+Co_2Ti(c)$, $Co_2Zr+CoTi+CoTi_2$, $CoTi_2+\beta(Ti,Zr)+M$, $\beta(Ti)+\alpha(Ti)+\beta(Ti,Zr)$, $\beta(Ti,Zr)+CoTi_2+\beta(Ti)$, $Co_2Zr+M+CoTi_2$, $Co_2Zr+N+M$, $Co_{23}Zr_6+Co_2Zr+Co$, $Co_2Zr+CoZr+CoZr_2$, $Co_2Zr+N+CoZr_2$, $CoZr_2+N+\beta(Ti,Zr)$, $M+N+\beta(Ti,Zr)$, $CoZr_2+\beta(Ti,Zr)+CoZr_3$ and $CoZr_3+\beta(Ti,Zr)+\alpha(Zr)$. The solid solubility of Ti inCo_2Zr, $CoZr_2$ and $CoZr_3$ is about 10.7 at.% Ti,1.9 at.% Ti and 4.3 at.% Ti, and that of Zr in $TiCo_3$, $TiCo_2(h)$, $TiCo_2(c)$, TiCo and Ti_2Co is about 0.9 at.% Zr, 8.4 at.% Zr, 6.0 at.% Zr, 7.5 at.% Zr and 16.0 at.% Zr, respectively. Two ternary phases are observed.

KEYWORDS

Intermetallics;
Co-Ti-Zr;
Phase diagrams;
Diffusion.

INTRODUCTION

Hydrogen-storage alloys are being used in various applications, e.g. hydrogen-fuelled transportation, hydrogen purification, secondary batteries, heat storage and heat pumps. At present, many researchers have been investigated the hydrogen storage properties of various metal hydride families such as the rare earth-based AB_5 type alloys[1, 2], the AB_2 type alloys[3-4], the Mg-based alloys[5-14], the V-based alloys[15] and the Ti–V-based multiphase alloys[16-21]. However, each type of alloy has its shortcomings. For example, the Zr-based AB_2 type alloys such as ZrV2, ZrCr2 and ZrFe2 are too stable to be practically used in reversible hydrogen storage. Fortunately, Hydrogen storage properties could be improved by adding some elements, including Mn[22-24], Ni[25-29], Co[18, 30-32] and Cu[33-35], etc. Although much attention has been paid to the properties of hydrogen storage alloys, study on the understanding of the phase diagrams in the Ti-Zr-Co-Fe-Mn-Cr-Ni-Cu-V system is also necessary for the design (optimal compositions) and fabrication (forming methods and heat-treatment conditions). Therefore, it is of theoretical importance to investigate the phase relationships of the Co-Ti-Zr alloy system.

The phase diagrams of all boundary binaries in the Co-Ti-Zr system have been well investigated. In

Ref.[36], the Zr-Ti system without any compounds was reported and the Co-Zr system shows the presence of five intermediate phases, i.e. $Co_{23}Zr_6$、Co_2Zr、CoZr、$CoZr_2$ and $CoZr_3$. In the Co-Ti system, five intermetallic compounds, Co_3Ti, h-Co_2Ti, c-Co_2Ti, CoTi and $CoTi_2$ occur besides the terminal solution phases, such as α-(Ti), β-(Ti), α-(Co) and ε-(Co)[37]. Recently thermodynamic modeling of the Co-Ti system was performed by Dupin et al[38], and many different solution phases are present, A1, L12 (Co_3Ti), A2, B2 (CoTi), A3, C15 (c-Co_2Ti) and C36 (h-Co_2Ti). A1 and L12, A2 and B2, exhibit an order/disorder relation, A1 and L12 are in equilibrium in the Co-rich side of the diagram. The structural data for the intermetallic compounds in Co-Ti-Zr systems are given in TABLE 1.

Up to now, to the best of our knowledge, very little work has been done about the phase equilibria in the Co-Ti-Zr ternary system. In present work, the phase equilibria in the Co-Ti-Zr system at 1023K were investigated by means of diffusion-triple approach.

EXPERIMENTAL DETAILS

The Co-Ti-Zr diffusion triple specimen was prepared from blocks of pure metals: Co (purity 99.9%) and Zr (purity 99.9%) and Ti (purity 99.5%). Firstly, to make a Co-Ti diffusion couple, the Ti and Co blocks were diffusionally welded under 4.5MPa pressure in argon flow at 1023K for 15 minutes then cooled to ambient temperature. Subsequently, the Co-Ti-Zr diffusion triple was assembled from the obtained Co-Ti couple and pure Zr block by diffusion welding under 4.5MPa pressure at 1023K in argon flow for 15 minutes. Finally, the triple was encapsulated in an evacuated quartz tube backfilled with pure argon and annealed at 1023K for 1680 hours. The flow chart for making the Co-Ti-Zr diffusion triple is shown in Figure 1.

The obtained diffusion triple was ground, polished and examined by electron probe microanalysis (EPMA) (JX-8800R, Japan, electron Optics Ltd., Tokyo) under the operation condition of 20kV voltage, 2×10^{-8}A current and a 40^o take-off angle.

RESULTS AND DISCUSSION

The back-scattered electron (BSE) images of the Co-Ti-Zr diffusion-triple annealed at 873K are shown in Figure 2, and Figure 3 shows the Schematic diagram of the 1023 K diffusion triple. The numbered triple nodes (1 to 17) represent ternary equilibria existing in the Co-Ti-Zr system. The phase boundary between c-Co_2Ti and h-Co_2Ti is not visible and therefore drawn as a dashed line at the middle of the figure.

Intermetallic compounds form as a result of ex-

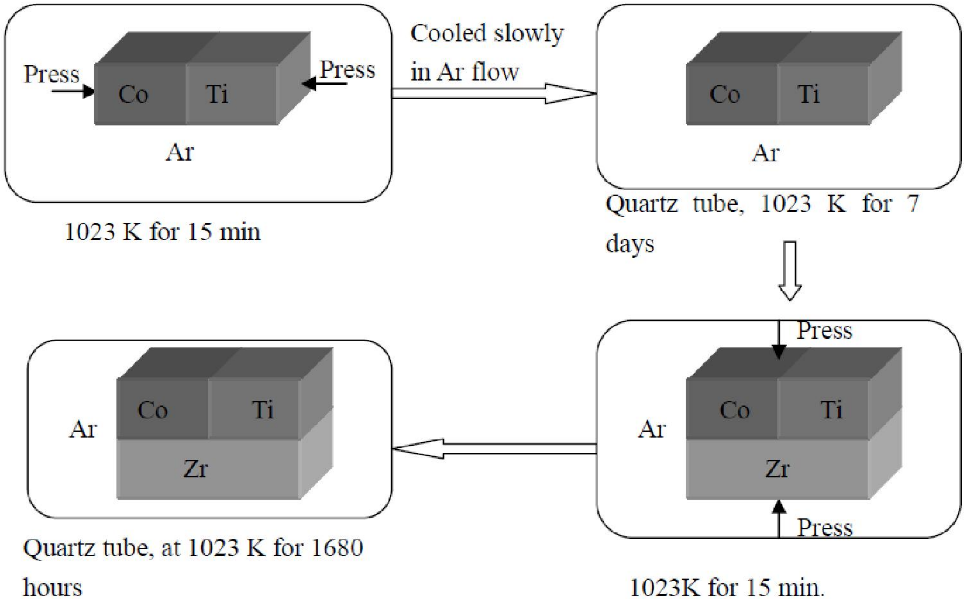

Figure 1 : Flow chart for making the Co-Ti-Zr diffusion triple

TABLE 1 : Solid phases and their crystal structures in the Co-Ti-Zr system

Phase	Struturbericht designation	Prototype	Pearson symbol	Space group	References
α(Ti,Zr)	A3	Mg	hP2	$P6_3/mmc$	[39]
β(Ti,Zr)	A2	W	cI2	$Im\bar{3}m$	[39]
$CoTi_2$	$E9_3$	Fe_3W_3C	cF96	$Fd\bar{3}m$	[40]
CoTi	B2	CsCl	cP2	$Pm\bar{3}m$	[40]
Co_2Ti(c)	C15	Cu_2Mg	cF24	$Fd\bar{3}m$	[40]
Co_2Ti(h)	C36	$MgNi_2$	hP24	$P6_3/mmc$	[40]
Co_3Ti	L12	Au_3Cu	cP4	$Pm\bar{3}m$	[40]
ε(Co)	A3	Mg	hP2	$P6_3/mmc$	[40]
α(Co)	A1	Cu	cF4	$Fm\bar{3}m$	[40]
$Co_{11}Zr_2$	unkown	unkown	unkown	unkown	[41]
$Co_{23}Zr_6$	$D8_a$	$Mn_{23}Th_6$	cF116	$Fm\bar{3}m$	[41]
Co_2Zr	C15	Cu_2Mg	cF24	$Fd\bar{3}m$	[41]
CoZr	B2	CsCl	cP2	$Pm\bar{3}m$	[41]
$CoZr_2$	C16	Al_2Cu	tI12	I4/mcm	[41]
$CoZr_3$	$E1_a(D0_{19})$	$Re_3B(Ni_3Sn)$	oC16(hP8)	Cmcm($P6_3/mmc$)	[41]

tensive interdiffusion among Co, Ti, Zr during long-term heat treatment. It is obvious that no layers of compounds in the Ti-Zr side, while there are five layers of compounds, :$Co_{23}Zr_6$, Co_2Zr, CoZr, $CoZr_2$ and $CoZr_3$ in the Co-Zr side, and five diffusion layers of $TiCo_3$, $TiCo_2$(h), $TiCo_2$(c), TiCo and Ti_2Co in the Co-Ti side, which is in good agreement with binary phase diagrams of the Ti-Zr[36], Co-Zr[36] and Co-Ti[37, 38]. It should be pointed out here that c-Co_2Ti and h-Co_2Ti could not be distinguished simply by color contrasts in Figure 2 due to the small different atomic weight of these phases, but we can detect the c-Co_2Ti and h-Co_2Ti by EPMA depends on the discontinuity of the composition in the two-phase region. As a result, the phase boundary between these two "Co_2Ti" phases is drawn with a dashed line.

TABLE 2 lists the tie-lines data obtained by EPMA, all the experiment data were taken from the couple cross-section along the phase boundary. As shown in TABLE 2, the solid solubility of Ti inCo_2Zr, $CoZr_2$ and $CoZr_3$ is about 10.7 at.% Ti,1.9 at.% Ti and 4.3 at.% Ti, and that of Zr in $TiCo_3$, $TiCo_2$(h), $TiCo_2$(c), TiCo and Ti_2Co is about 0.9 at.% Zr, 8.4 at.% Zr, 6.0 at.% Zr, 7.5 at.% Zr and 16.0 at.% Zr, respectively.

It's important to note that, as shown in Figure 2 (b), two ternary phase layers were appeared according to the analysis of EPMA (we named them as "M" and "N'). Base on the component analysis, all of them have some range of constituent. As to ternary phase M, the range of Co constituent is about 25.8 at.% to 32.1 at.% and that of Ti is about 40.3 at.% to

TABLE 2 : Extrapolated compositions of the phases in equilibrium at 1023K

Co/Co$_3$Ti				**Co$_2$Zr/CoZr**			
Co	**Ti**	**Co**	**Ti**	**Co**	**Ti**	**Co**	**Ti**
99.5	0.5	77.7	22.2	69.9	0	50.1	0
99.8	0.2	78.0	21.5	**CoZr /CoZr$_2$**			
99.5	0.5	77.8	22.2	**Co**	**Ti**	**Co**	**Ti**
99.5	0.5	78.3	21.7	49.8	0	35.5	0
99.4	0.6	77.6	22.4	**Co$_2$Zr/CoTi**			
98.3	0.1	78.5	21.4	**Co**	**Ti**	**Co**	**Ti**
Co$_2$Zr/ CoTi$_2$				69.4	8.4	50.0	48.9
Co	Ti	Co	Ti	69.1	8.2	50.1	48.5
68.8	7.8	34.0	50.3	**CoTi$_2$/M**			
Co$_3$Ti/Co$_2$Ti(h)				**Co**	**Ti**	**Co**	**Ti**
Co	**Ti**	**Co**	**Ti**	33.6	50.3	31.6	42.6
75.4	24.4	72.4	19.0	33.9	50.1	32.0	41.6
74.8	25.2	69.8	30.2	33.9	0	26.7	0
75.2	24.8	72.3	19.7	33.7	0.1	27.0	0.1
Co$_3$Ti/Co$_2$Zr				**Co/Co$_{23}$Zr$_6$**			
Co	**Ti**	**Co**	**Ti**	**Co**	**Ti**	**Co**	**Ti**
77.8	21.3	75.6	10.7	100.0	0	81.2	0
75.9	23.7	73.8	9.9	99.6	0	81.8	0
Co$_2$Ti(c)/ CoTi				**Co$_{23}$Zr$_6$/ Co$_2$Zr**			
Co	**Ti**	**Co**	**Ti**	**Co**	**Ti**	**Co**	**Ti**
67.4	26.5	50.3	49.1	79.4	0	72.8	0
67.9	27.5	50.1	49.5	80.0	0	72.5	0
67.0	33.0	53.0	47.0	**M/ β (Ti,Zr)**			
CoTi/ CoTi$_2$				**Co**	**Ti**	**Co**	**Ti**
Co	**Ti**	**Co**	**Ti**	**26.7**	**45.7**	**4.4**	**68.2**
48.5	50.6	33.8	50.7	26.3	46.0	3.8	66.5
48.1	51.3	33.7	51.7	25.8	43.8	3.6	38.9
48.3	51.7	33.6	66.4	26.3	43.7	2.8	52.5
CoTi$_2$/β(Ti,Zr)				**N/β(Ti,Zr)**			
Co	**Ti**	**Co**	**Ti**	**Co**	**Ti**	**Co**	**Ti**
33.2	50.8	4.7	68.2	29.8	31.5	3.1	32.6
33.4	51.4	5.1	68.9	29.9	32.9	2.8	33.6
CoTi$_2$/β(Ti)				28.8	30.7	2.8	31.7
Co	**Ti**	**Co**	**Ti**	29.2	30.5	3.4	31.2
33.3	66.7	9.1	90.8	**M/N**			
CoZr$_3$/β(Ti,Zr)				**Co**	**Ti**	**Co**	**Ti**
Co	**Ti**	**Co**	**Ti**	28.3	41.9	30.7	33.6
26.3	0.7	1.7	4.1	27.9	41.7	29.7	33.5

<table>
<tr><th colspan="4">Co_2Zr/M</th><th colspan="4">$CoZr_3$/α(Zr)</th></tr>
<tr><th>Co</th><th>Ti</th><th>Co</th><th>Ti</th><th>Co</th><th>Ti</th><th>Co</th><th>Ti</th></tr>
<tr><td>67.3</td><td>7.0</td><td>32.3</td><td>40.1</td><td>25.2</td><td>0</td><td>0.8</td><td>0</td></tr>
<tr><th colspan="4">β(Ti) /α(Ti)</th><td>26.4</td><td>0</td><td>0.9</td><td>0</td></tr>
<tr><th>Co</th><th>Ti</th><th>Co</th><th>Ti</th><td>26.4</td><td>0</td><td>0.5</td><td>0</td></tr>
<tr><td>5.3</td><td>94.2</td><td>0.2</td><td>99.5</td><td>25.8</td><td>0.5</td><td>0.8</td><td>0.3</td></tr>
<tr><th colspan="4">Co_2Ti(h)/ Co_2Ti (c)</th><th colspan="4">Co/Co_2Zr</th></tr>
<tr><th>Co</th><th>Ti</th><th>Co</th><th>Ti</th><td>Co</td><td>Ti</td><td>Co</td><td>Ti</td></tr>
<tr><td>71.0</td><td>19.7</td><td>68.7</td><td>26.3</td><td>99.2</td><td>0.7</td><td>75.7</td><td>9.5</td></tr>
<tr><th colspan="4">Co_2Ti(h)/Co_2Zr</th><th colspan="4">$CoZr_2$/β(Ti,Zr)</th></tr>
<tr><th>Co</th><th>Ti</th><th>Co</th><th>Ti</th><th>Co</th><th>Ti</th><th>Co</th><th>Ti</th></tr>
<tr><td>72.0</td><td>19.6</td><td>71.8</td><td>8.5</td><td>33.2</td><td>1.9</td><td>2.2</td><td>10.7</td></tr>
<tr><th colspan="4">Co_2Zr/M</th><th colspan="4">$CoZr_2$/ $CoZr_3$</th></tr>
<tr><th>Co</th><th>Ti</th><th>Co</th><th>Ti</th><th>Co</th><th>Ti</th><th>Co</th><th>Ti</th></tr>
<tr><td>68.3</td><td>3.1</td><td>32.1</td><td>29.7</td><td>34.0</td><td>0</td><td>27.0</td><td>0</td></tr>
</table>

46.0 at.%. Similarly to ternary phase of N, the range of Co constituent is about 29.0 at.% to 32.1 at.% and that of Ti is about 30.5 at.% to33.6 at.% (As shown TABLE 2). On the other hand, we have not detected the ternary phase of $Co_{66}Ti_{17}Zr_{17}$[42].

It is worthwhile noting that the local equilibrium is only reached at the phase interface, not in the entire diffusion zone. Away from the interface, each infinitely thin layer of such a diffusion zone is not in thermodynamic equilibrium with the neighboring layers—the chemical potential (activity) gradient still exists at neighboring layers and will continue to drive diffusion if the sample is annealed for longer time. The local equilibrium has been maintained only at the interface, which serves as the base of applying diffusion couple techniques for determining equilibrium phase diagrams. The existence and establishment of the local equilibrium at phase interfaces in diffusion couples have been demonstrated by many experiments over the past several decades[43, 44]. The establishment of local equilibrium at phase interfaces in the diffusion multiple is not any different from that in diffusion couples.

The experimental results may contain errors directly attributable to the nature of the sample, such as cracks, grain boundaries, etc. may also render the interpretation of diffusion couple experiments cumbersome. Another source of error is in the experimental measurements themselves. The difficulties connected with the accurate determination of the boundary concentrations in the reaction zone are a problem for both semi-infinite and finite diffusion couple techniques. Thirdly, the determination of a chemical composition with EPMA has an inherent experimental error associated with data counting statistics and data correction procedures. Finally, accurate microprobe analysis near the interfaces is sometimes very difficult owing to fluorescence effects.

Generally, the tie-triangles in the isothermal section can be defined by measuring the compositions of phases near triple points. Because of the electron scattering effect and the very small phase areas involved near the triple points, the EPMA measurements are taken at a short distance along the lines perpendicular to and across the phase interfaces. Extrapolation of the composition profiles to the interface positions could show the phase compositions in equilibrium. After each tie-line being extrapolated to the tri-junction point, tie-triangle representing three-phase field can be obtained. An isothermal section of the Co-Ti-Zr system at 1023K was established as shown in Figure 4. The isothermal section consists of nine three-phase fields, namely $Co_3Ti+Co_2Zr+Co_2Ti(h)$, $Co_2Zr+Co_2Ti(h)+Co_2Ti(c)$, $Co_3Ti+Co+Co_2Zr$, $Co_2Zr+CoTi+Co_2Ti(c)$, $Co_2Zr+CoTi+CoTi_2$, $CoTi_2+\beta(Ti,Zr)+M$, β(Ti) +α(Ti)+ β(Ti,Zr), $\beta(Ti,Zr)+CoTi_2+\beta(Ti)$, $Co_2Zr+M+CoTi_2$,

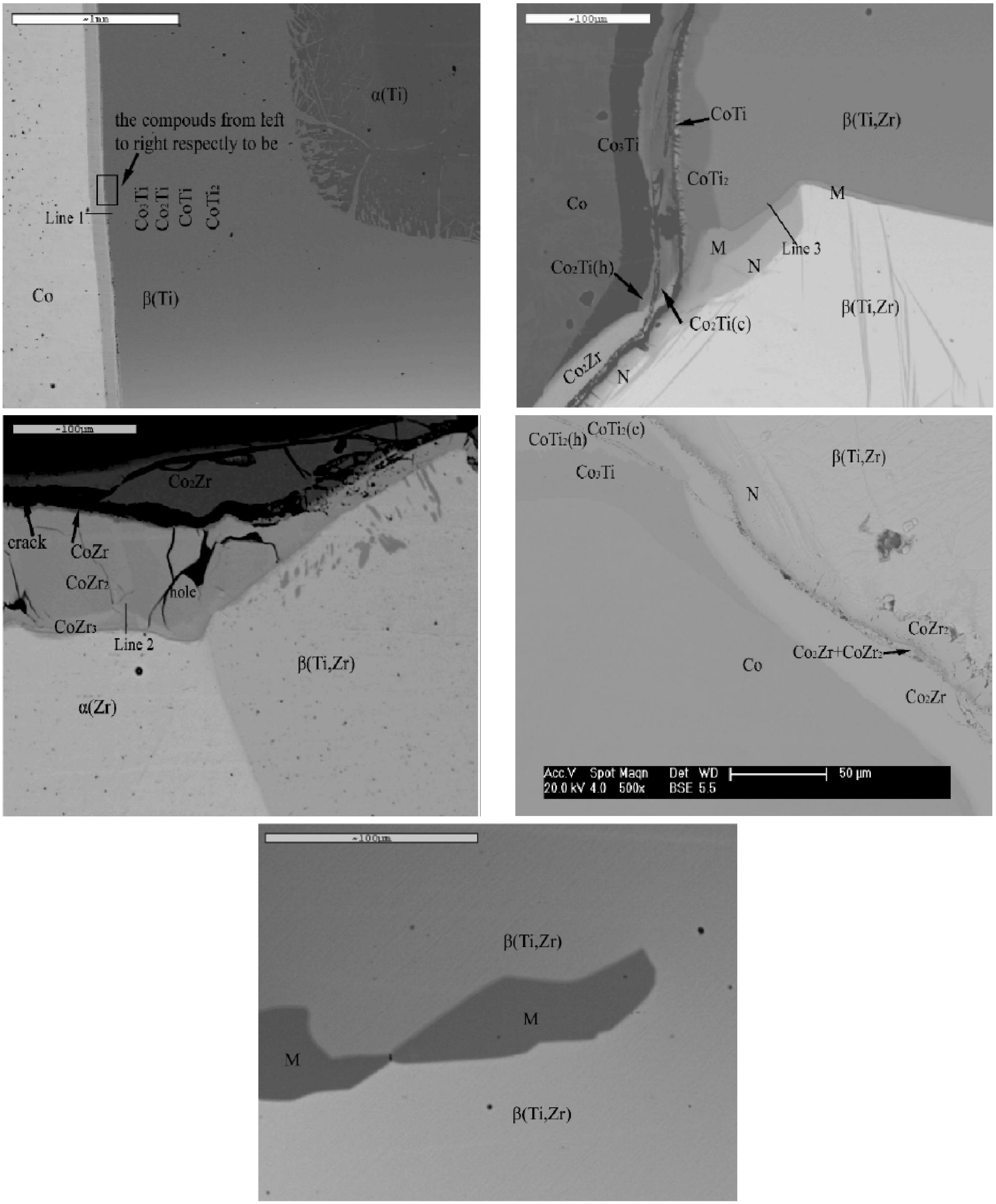

Figure 2 : Backscattered electron images of the Co-Ti-Zr diffusion triple annealed at 1023 K. (a) Two-phase field of Co-Ti, (b) Three-phase field, (c) Two-phase field of Co-Zr, (d) Two-phase field of Co-Zr of Ti-rich, (e) Three-phase boundary field.

Co_2Zr+N+ M, $Co_{23}Zr_6$+Co_2Zr +Co, Co_2Zr+ CoZr+$CoZr_2$, Co_2Zr+N+$CoZr_2$, $CoZr_2$+N+ β(Ti,Zr),

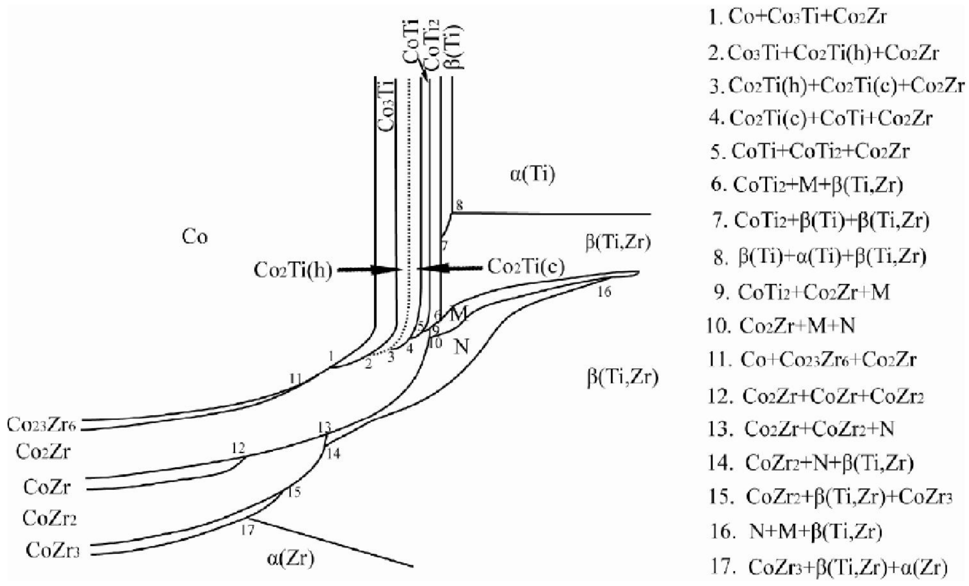

Figure 3 : Schematic diagram of the 1023 K diffusion triple. The numbered triple nodes (1 to 17) represent ternary equilibria existing in the Co-Ti-Zr system. The phase boundary between c-Co_2Ti and h-Co_2Ti is not visible and therefore drawn as a dashed line at the middle of the figure.

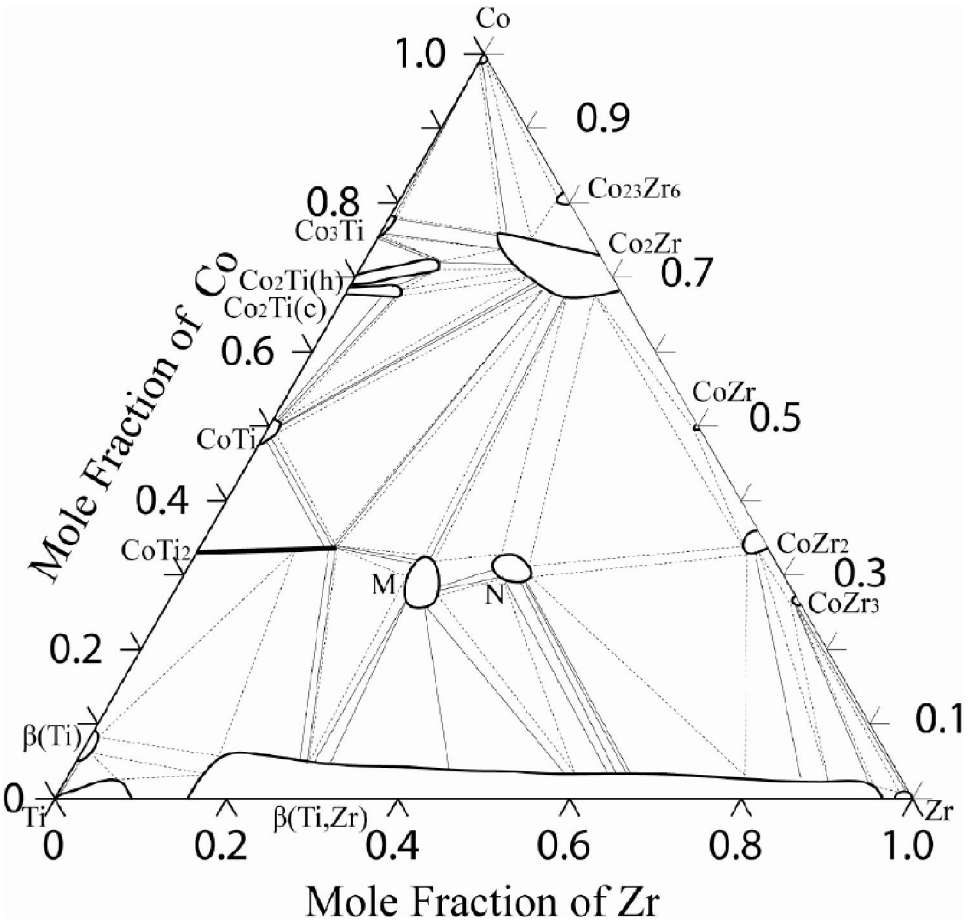

Figure 4 : The isothermal section of the Co-Ti-Zr ternary system at 1023K

M+N+β(Ti,Zr), $CoZr_2$+β(Ti,Zr)+ $CoZr_3$ and $CoZr_3$+ β(Ti,Zr)+α(Zr). The tie-lines are defined from the EPMA line profiles by taking advantage of the local equilibrium at interfaces formed among the phases.

So, the three-phase equilibrium concentrations are just estimated values at this phase diagram, hence the corresponding tie-triangles are drawn as dashed lines.

CONCLUSIONS

The isothermal section of the Co-Ti-Zr ternary system at 1023K was determined by means of diffusion triple and EPMA technique. 17 three-phase equilibria were obtained. All of the Co-Zr and Co-Ti binary phases show large ternary solubility. the solid solubility of Ti inCo_2Zr, $CoZr_2$ and $CoZr_3$ is about 10.7 at.% Ti,1.9 at.% Ti and 4.3 at.% Ti, and that of Zr in $TiCo_3$, $TiCo_2$(h), $TiCo_2$(c), TiCo and Ti_2Co is about 0.9 at.% Zr, 8.4 at.% Zr, 6.0 at.% Zr, 7.5 at.% Zr and 16.0 at.% Zr, respectively, and two ternary phases were found.

ACKNOWLEDGEMENT

This work was supported by the science Foundation of Hunan Education Department (No, 11C0620), the Science Foundation of Hunan (No, 12JJ3045) and project of the Key Discipline Development of Hunan.

REFERENCES

[1] H.G.Pan, J.X.Ma, C.S.Wang, C.P.Chen, Q.D.Wang; Electrochim Acta., **44**, 3977 **(1999)**.
[2] S.D.Wu, Y.Q.Zhu, C.Li, S.Xiao, H.X.Wang; J.Alloys Compd., **582**, 289 **(2014)**.
[3] A.Leela Mohana Reddy, S.Ramaprabhu; J Alloys Compd., **460**, 268 **(2008)**.
[4] F.C.Ruiz, E.B.Castro, S.G.Real, H.A.Peretti, A.Visintin, W.E.Triaca; Int.J.Hydrogen Energy., **33**, 3576 **(2008)**.
[5] M.Anik, I.Akay, S.Topcu; Int.J.Hydrogen Energy., **34**, 5449 **(2009)**.
[6] L.Z.Ouyang, J.M.Huang, H.Wang, Y.J.Wen, Q.A.Zhang, D.L.Sun, M.Zhu; Int.J.Hydrogen Energy., **38**, 2973 **(2013)**.
[7] L.Z.Ouyang, J.M.Huang, C.J.Fang, H.Wang, J.W.Liu, Q.A.Zhang, D.L.Sun, M.Zhu; J Alloys Compd., **580**, S317 **(2013)**.
[8] Y.F.Liu, H.G.Pan, M.X.Gao, R.Li, Y.Q.Lei; J.Alloys Compd., **376**, 296 **(2004)**.
[9] Y.F.Liu, H.G.Pan, M.X.Gao, Y.F.Zhu, H.W.Ge, S.Q.Li, Y.Lei; Acta Metallurgica Sinica., **39**, 666 **(2003)**.
[10] H.G.Pan, S.Ma, J.Shen, J.J.Tan, J.L.Deng, M.X.Gao; Int.J.Hydrogen Energy., **32**, 2949 **(2007)**.
[11] S.Ma, M.X.Gao, M.X.Gao, R.Li, H.G.Pan, Y.Q.Lei; J.Alloys Compd., **457**, 457 **(2008)**.
[12] H.G.Pan, Y.G.Yue, M.X.Gao, X.F.Wu, N.Chen, Y.Q.Lei, Q.D.Wang; J.Alloys Compd., **397**, 269 **(2005)**.
[13] Y.J.Yang, Y.F.Liu, Y.Zhang, Y.Li, M.G Gao, H.G Pan; J.Alloys Compd., **585**, 674 **(2014)**.
[14] Y.P.Fan, X.Y.Peng, T.C.Su, H.Bala, B.Z.Liu; J.Alloys Compd., **596**, 113 **(2014)**.
[15] C.L.Wu, Y.G.Yan, Y.G.Chen, M.D.Tao, X.Zheng; Int.J.Hydrogen Energy., **33**, 93 **(2008)**.
[16] Y.F.Zhu, H.G.Pan, M.X.Gao, J.X.Ma, S.Q.Li, Q.D.Wang; Int.J.Hydrogen Energy., **27**, 287 **(2002)**.
[17] Y.F.Liu, S.H.Zhang, R.Li, M.X.Gao, K.Zhong, H.Miao.H.G.Pan; Int.J.Hydrogen Energy., **33**, 728 **(2008)**.
[18] H.Miao, M.X.Gao, Y.F.Liu, D.Zhu, H.G.Pan; J.Power Sources., **184**, 627 **(2008)**.
[19] M.X.Gao, H.Miao, Y.Zhao, Y.F.Liu, H.G.Pan; J.Alloys Compd., **484**, 249 **(2009)**.
[20] H.G.Pan, R.Li, Y.F.Liu, M.X.Gao, H.Miao, Y.Q.Lei, Q.D.Wang; J.Alloys Compd., **463**, 191 **(2008)**.
[21] S.Basak, K.Shashikala, S.K.Kulshreshtha; Int.J.Hydrogen Energy., **33**, 350 **(2008)**.
[22] S.L.Li, H.H.Cheng, X.X.Deng, W.Chen, D.M.Chen, K.Yang; J.Alloys Compd., **460**, 186 **(2008)**.
[23] E.D.Wu, W.H.Li, J.Li; Int.J.Hydrogen Energy., **37**, 1509 **(2012)**.
[24] R.X.Liu, D.Book; Int.J.Hydrogen Energy., **39**, 2194 **(2014)**.
[25] A.Jain, R.K.Jain, S.Agarwal, V.Ganesan, N.P.Lalla, D.M.Phase, I.P.Jain; Int.J.Hydrogen Energy., **32**, 3965 **(2007)**.
[26] A.Jain, G.Agarwal, I.P.Jain; J.Alloys Compd., **480**, 325 **(2009)**.
[27] Y.Zhao, M.G.Gao, Y.F.Liu, L.Huang, H.G Pan; J.Alloys Compd., **496**, 454 **(2010)**.
[28] Y.F.Liu, Y.H.Cao, L.Huang, M.G.Gao, H.G Pan; J.Alloys Compd., **509**, 675 **(2011)**.
[29] H.P.Yuan, Z.Y.Zou, Z.N.Li, J.H.Ye, X.M.Guo,L.J.Jiang, S.M.Wang, X.P.Liu; Int.J.Hydrogen Energy., **38**, 7881 **(2013)**.
[30] A.Jain, R.K.Jain, G.Agarwal, I.P.Jain; J.Alloys Compd., **438**, 106 **(2007)**.

[31] H.Y.Shao, J.Matsuda, H.W.Li, E.Akiba, A.Jain, T.Ichikawa, Y.Kojima; Int.J.Hydrogen Energy., **38**, 7070 **(2013)**.

[32] C.C.Cormos; Int.J.Hydrogen Energy., **37**, 5637 **(2012)**.

[33] R.Parimala, M.V.Ananth, S.Ramaprabhub, M.Raju; Int.J.Hydrogen Energy., **29**, 509 **(2004)**.

[34] Y.H.Zhang, C.Li, Y.Cai, F.Hu, Z.H.Liu, S.H.Guo; J.Alloys Compd., **584**, 81 **(2014)**.

[35] X.Tan, M.Danaie, W.P.Kalisvaart, D.Mitlin; Int.J.Hydrogen Energy., **36**, 2154 **(2011)**.

[36] T.B.Massalski (Ed.); Binary alloy phase diagrams, ASM International, Materials Park, OH, USA, **(1990)**.

[37] J.L.Murray; Phase diagram of binary titanium alloys, J.L.Murray Ed., ASM International, Materials Park, OH, 59 **(1987)**.

[38] G.Cacciamani, R.Ferro, I.Ansara, N.Dupin; Intermetallics., **8**, 213 **(2000)**.

[39] J.L.Murray; ASM International, Metals Park, OH, 340 **(1987)**.

[40] J.L.Murray; ASM International, Materials Park, OH, 59 **(1987)**.

[41] S.K.Bataleva, V.V.Kuprina, V.V.Burnasheva, V.Ya.Markiv, G.N.Ronami, S.M.Kuznetsova; Vestn.Mosk.Univ., **5**, 577 **(1970)**.

[42] Z.Blazina, R.Trojko; J.Less-Comm.Metals., **133**, 277 **(1987)**.

[43] F.J.J.Van Loo; Prog Solid State Chem., **20**, 47 **(1990)**.

[44] A.A.Kodentsov, G.F.Bastin, F.J.J.van Loo; J.Alloys Compd., **320**, 207 **(2001)**.